2. Literature Review

## 2.1. Structure and properties of carbon nanotubes

2.1.1. Structure

To determine the structure of the carbon nanotube, scientists used the two spatial vectors to depict the feature of CNTs which is expressed as:

$$Ch = na1 + ma2 \equiv (n,m).$$

where the Ch is chiral vector, a1 and a2 are the unit vectors of graphene sheet with n and m being integers. Figure 2-1 shows the chiral vector representation on the 2D graphene sheet. It indicates an angle θ between Ch and a1 called the chiral angle with respect to the zigzag axis at θ= 0o. The diameter (d) of CNT and the chiral angle θ can be expressed in term of

$$d = \frac{a\sqrt{m^2 + mn + n^2}}{\pi}$$

$$\theta = \sin^{-1}\left[\frac{\sqrt{3}m}{2\sqrt{n^2 + mn + m^2}}\right]$$
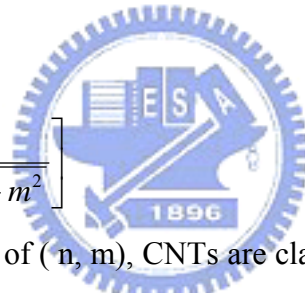
Depending on the chiral vetor of (n, m), CNTs are classified into three forms, namely the zigzag, armchair and chiral CNTs. They are corresponding to the chiral vectors of (n, 0), (n, n) and (n, m), respectively, as shown in figure 2.2. Details of structure parameter to describe and classify carbon nanotube are listed in Table 2.1.
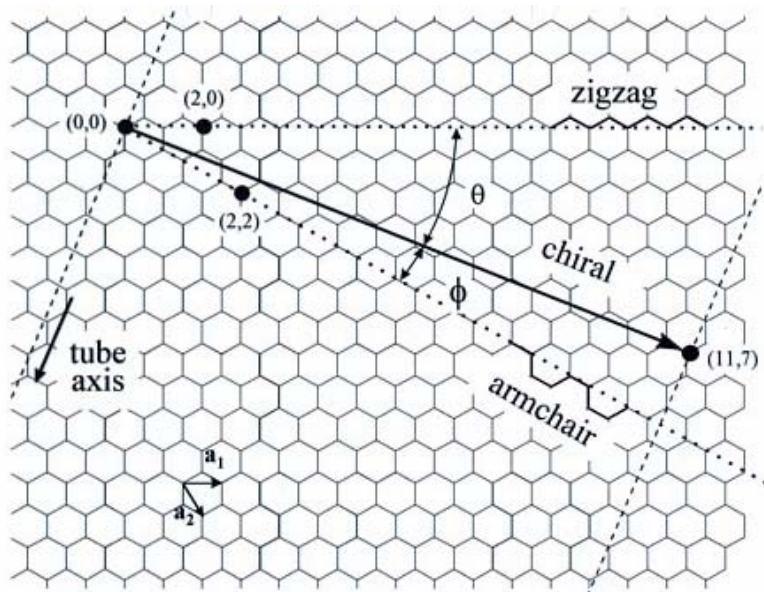
Figure2.1: A scheme of chiral vector on 2D grapheme sheet. Ch: the chiral vector presented as Ch = na1+ma2 ≡ (n, m), a1 and a2: the unit vectors of graphene sheet with n and m being integers, θ=chiral angle [42].
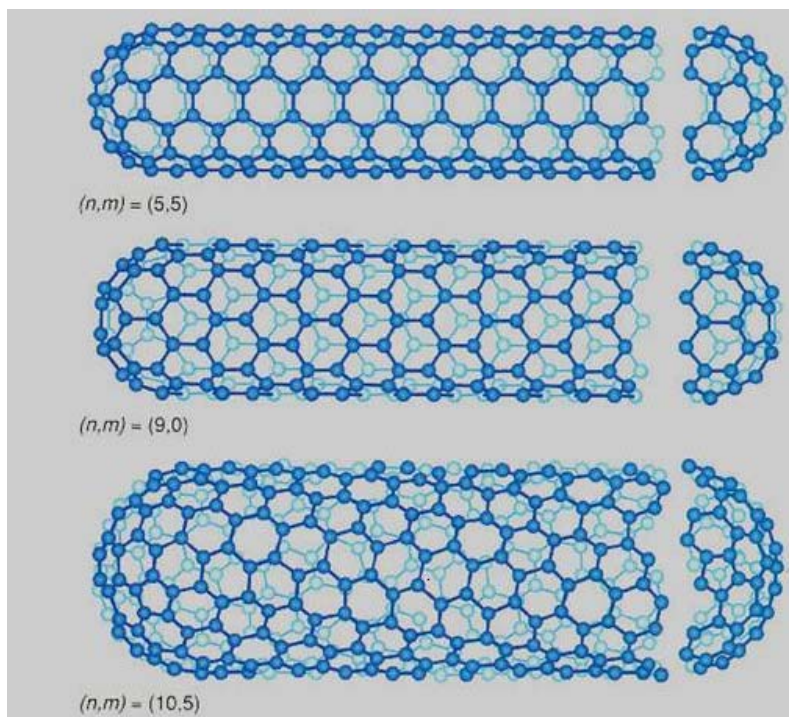

Figure2.2:Carbon nanotubes with chiral vectors of (a) armchair (n, n), (b) zigzag (n, 0), and chiral (n, m) [42].

Table 2.1: *Structure parameter of carbon nanotubes*

Name	formula	Value
Carbon-carbon distance		$1.42\,\overset{\circ}{A}$
Length of units vectors	$\sqrt{3}\,a$	$2.46\,\overset{\circ}{A}$
Chiral vector	$C_h=na_1+ma_2=(n,m)$	n,m :integers 1.m=n:armchair 2.m=0 or n=o :zigzag 3.others :chiral
Diameter of nanotube	$d=\dfrac{L}{\pi}=\dfrac{\sqrt{n^2+m^2+nm}}{\pi}a$	SWNT:1.2~1.4nm MWNT:
Chiral angle	$\sin\theta=\dfrac{\sqrt{3}\,m}{2\sqrt{n^2+m^2+nm}}$ $\cos\theta=\dfrac{2n+m}{2\sqrt{n^2m^2+nm}}$ $\tan\theta=\dfrac{\sqrt{3}\,m}{2n+m}$	$0\le|\theta|\le 30°$
Lattice constant		17A(SWNT)
Lattice parameter		(10,10)armchair:16.78A (17,0) zigzag:16.52A (12,6)chiral:16.52A
Interlayer spacing		(n,n)armchair:3.38A (n,0) zigzag:3.41A (2n,n)chiral:3.39A

2.1.2. Properties

2.1.2.1. Electrical properties

Perfect nanotubes are either metallic or semiconducting, depending on their helicity indices (n,m)[2.1]. Theoretical calculations have predicted that all the electrical conductivity of armchair tubes are metallic, whereas the zigzag and chiral tubes are either metallic or semiconducting depending on its chirality. The most significant property of semiconducting nanotubes is that their band gap depends on diameter, and it is found to be about 0.9eV/D(eV/nm), where D is the outer diameter of tube [2.1]. There have two possibilities for the chiral and zigzag nanotubes to act as metals or semiconductors:

(a) If n-m = 3q, q $\ne$ 0, the CNTs are semiconducting

(b) If n-m $\neq$ 3q, the CNTs are semimetal.

Detail descriptions of the three forms of nanotubes were listed in Table 2.2.

Table 2.2: *Electrical properties of carbon nanotubes*

| Property	Carbon nanotube
Conductance Quantization	$(12.9k\Omega^{-1})$
Resistivity	$10^{-4}\Omega - cm$
Maximum current density	1013A/m2
Material classification	m-n=3k:(semiconductor)) m=n :(metallic) others:(semi-metal)

2.1.2.2. Mechanical properties

Nanotubes are strong and resilient. Their mechanical properties have been measured by stretching and bending. The Young's modules for MWNTs is found to vary with their radius [2.2-2.4]. For example, the Young's modules is about 1000GPa for CNTs with Φ <5nm.ForΦ~15nm, the tensible strength of CNT is about 150GPa. Simliar values have been measured for SWNT: Young's module is about 1000GPa, while tensible strength is about 150~180GPa. Details of mechanical properties and physical properties for nanotubes were listed in Table 2.3 and 2.4, respectively.

Table 2.3: *Mechanical properties of CNTs compared with other Materials [84]*

Materials	Young's modulus (GPa)	Tensile strength (GPa)	Density (g/cm^3)
SWNT	1054	100~150	1.3~1.4
MWNT	1200	100~150	2.6

Table2.4: *Physical properties of carbon nanotubes*

Property	Carbon nanotube
Atomic density(C atoms/cm3)	(10,10)armchair:1.33 (17,0) zigzag:1.34 (12,6)chiral:16.52
Atomic density(g/cm3)	(10,10)armchair:1.33 (17,0) zigzag:1.34 (12,6)chiral:1.40
Thermal conductivity(RT)(W/cm-K)[C]	~2000
Phonon mean free path(nm)	~100
Realaxation time(s)	~10^{-11}
Youngs modle(GPa)	~1000(SWNT) ~1280(MWNT)
Band gap(eV)	1. For (n,m):n-m is divisible by 3(metallic) =0 2. For(n,m):n-m is not divisible by 3(semiconducting)=~0.5
Resistivity(Ωcm)	~C10^{-4}
C-C Tight Bonding Overlap Energy	~2.5eV(SWNT)
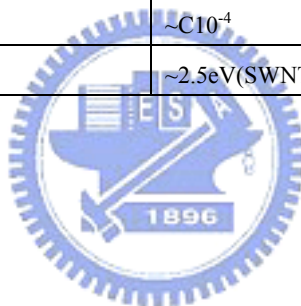
2.2. Nanofabrication of carbon nanotube

To date, arc-discharge [2.5-2.6], laser ablation [2.7], and (CVD) are the three main methods for nanotube production. Arc-discharge and laser ablation were the first methods that allowed fabrication of carbon nanotube with large yield. Both methods involve the condensation of hot gaseous carbon atoms generated from the evaporation of solid carbon materials. However, large amount of energy are consumed by these two methods making them suitable only in laboratory scale. The CVD method, which can be easily scaled up to industrial levels, is the most important method for nanotube production. Recent processes in the fabrication of carbon nanotube were focus on control of their diameter, orientation and alignment.

2.2.1. Arc discharge

Figure 2.3 shows the detail experimental for arc-discharge (also known as vaporization method). It was initially used for producing C60 fullerenes because of its simple configuration to undertake. For synthesizing nanotubes, two graphite rods were placed end to end. The distance between two rods is about 1 mm. A Cu chamber usually filled with inert gas (He or Ar) at low pressure (50~700 mbar) is used to enclose the whole assembly. A DC current (about 50 to 100 A) driven by applied voltage causes a high temperature discharge between the two electrodes. The discharge vaporizes the carbon rods and the products deposit on the other rod. Production yield depends on the uniformity of the plasma arc and the temperature of the deposition on the carbon electrode.
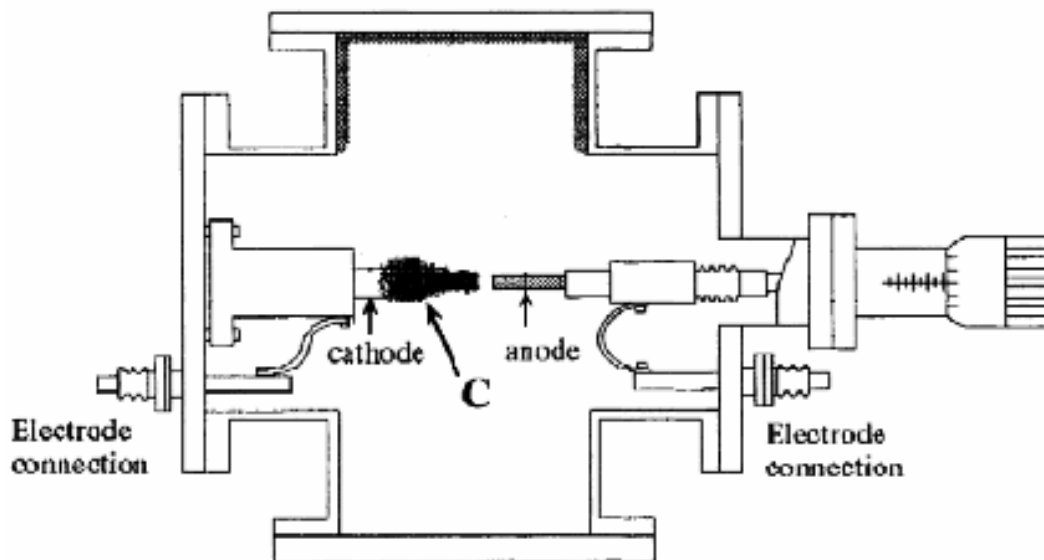
Figure 2.3: Schematic drawing of arc-discharge system. A DC current causes a high temperature discharge between the two electrodes. The discharge vaporizes the carbon rods and the products (indicated by symbol C) deposit on the other rod [43].

2.2.2. Laser abalation

It was firstly reported by Smalley's group in 1995. It is also called laser vaporization method. The Nd: YAG laser (continuous or pulse type) can be employed to bombard a target, where the target is composed of graphite or graphite with metal composition. The oven is at the pressure at 500 Torr, filled with the Ar or He gas. The vaporized species will deposit on the cooling copper finger or wire. If catalyst is used to assist CNT growth, the SWNT in 1-nm-diameter can be obtained. This method has higher yield than arc-discharge, but the drawback is the purity of product is not very good, meaning that it needs post-treatment to purify.

The Nd: YAG laser can be employed to bombard a target which is composed of graphite. The vaporized species will deposit on the cooling copper finger or wire. [2.44]

2.2.3. Chemical vapor deposition

The CVD method, which can be easily scaled up to industrial production levels, has become the most important commercial method for nanotube production. Chemical vapor deposition is used to describe reactions in which both solid and volatile

14

products are generated from a volatile precursor through chemical vapor deposition, and solid products are deposited on the substrate [2.8-2.9]. It has become a common method for thin-film growth on various substrate and is successful in making nanotube films, including SWNTs and MWNTs.

Another advantage is that it allowed more control over the morphology and surface structure of the produced nanotubes. With the CVD method, it is possible to produce nanotubes for fabricating nanoscale electronics. The CVD method can be divided into two categories: thermal CVD and PECVD (including ECR-CVD,ICP-CVD,MPCVD)

2.2.3.1. Thermal CVD

Figure 2-4 shows a schematic diagram of thermal CVD apparatus for synthesizing carbon nanotubes. Pyrolysis of hydrocarbon source was used to generate carbon atoms. This method is catalytic assisted CNTs growth method and the quality of CNTs is strongly depending on the pyrolysis temperature. The specimen is placed in a quartz boat with coated transition metals(such as Fe, Co, and Ni) on a substrate. The boat is positioned in a reaction furnace. Well-separated, nano-size catalytic metal particles are formed after etched with reaction gas(such as CH4,C2H2,NH3···) at temperatures ranging from 700℃ to 1100℃. Reaction gas outlet at the other end of the furnace. The CVD method is easy to deposit large area, uniform and good quality CNTs. However such a process is not compatible with integrated circuit process due to high reaction temperature over 650 ℃. Over the last years, several CVD methods have been developed and have the potential for industrial- scale preparation of nanotubes. Among them there are few different approaches shown to be promising: mrthaneCVD [2.10-2.13], HiPCO (High-Pressure Catalytic oxide) [2.14-2.15], COCVD, and alcohol CVD [2.16].

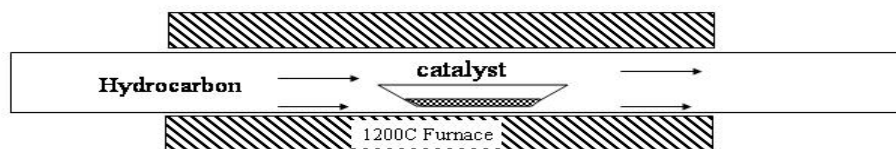Figure 2.4: Schematic drawing of thermal CVD system. Pyrolysis of hydrocarbon source (such as CH4, C2H2, NH3…) was used to generate carbon atoms. The specimen is placed in a quartz boat with coated transition metals (such as Fe, Co, and Ni) on a substrate. Well-separated, nano-size catalytic metal particles are formed after etched with reaction gas at temperatures ranging from 700℃ to 1100℃. [45]

2.2.3.2. PECVD(Plasma Enhance CVD)

Fig. 2.5 is a schematic drawing of PECVD apparatus. It has many advantages, including low energy consumed, compatible with IC process, high yield, controlled-alignment of CNTs. Scientists have focused on developing new process techniques to prepare well-aligned CNTs with PECVD. Depending on the mechanism of plasma excitation, PECVD can be classified into several different types including microwave plasma CVD (MPCVD), RF or DC bias excited plasma CVD (PECVD), microwave plasma assisted hot filament CVD (MP-HFCVD) and electron cyclotron resonance CVD (ECR-CVD).

The power supplies to discharge plasma are DC bias; radio frequency (RF) (13.56 MHz) and microwave (2.47 GHz) are typical of high frequency power supply. Using the plasma CVD process to produce CNTs can be prepared by applying decomposition of hydrocarbon (such as CH_4, C_2H_2) or monoxide and even decomposed of metal complex on various substrates that coated transition-metal film(such as Fe, Co, Ni). The commonly used microwave plasma CVD for fabricating CNTs can be ranked in terms of their working pressure, where MP-CVD or PE-HF-CVD and ECR-CVD were operated with the pressure range of P < 10-3 Torr and 10-1 < P < 100 Torr, respectively. The MPCVD, with the high density of plasma ball permits a contamination-free and a modification of plasma shape through tuning of the cavity.
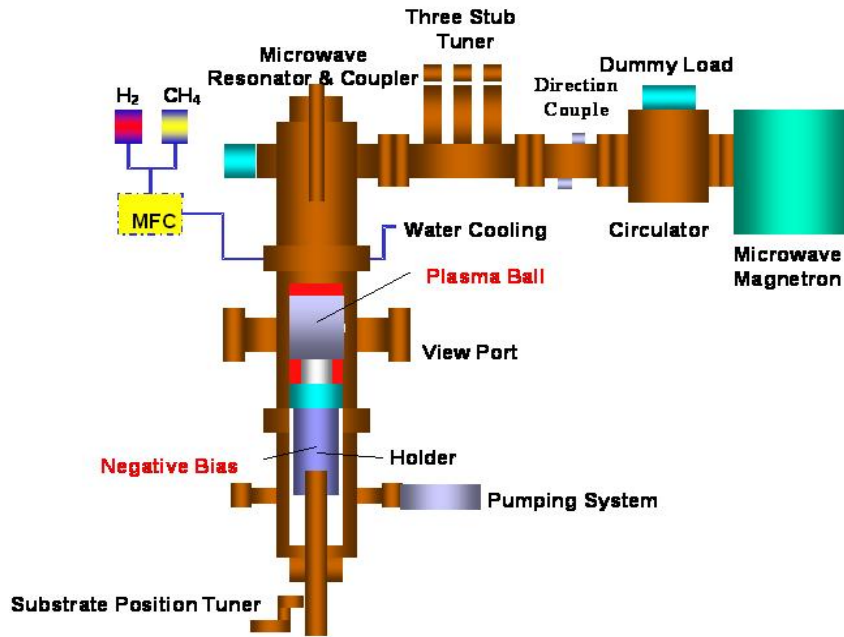
Figure 2.5: Schematic drawing of the MPCVD system used in our experiment [46].

2.3. Grown mechanisms of carbon nanotube synthesized by MPCVD

2.3.1. Growth with catalyst

2.3.1.1. Carbon diffusion through (on) catalyst paraticles.

Four stages seem to be useful in attemping to sketch out the growth mechanism of carbon nanotubes :

(1) First, metal particles (such as Fe, Co and Ni) resulted from the rupture of the surface which suffering the plasma etching. This pretreatment process leads to the formation of catalytic particles [2.39].

(2) Secondly, carbon atoms, dissociated from the hydrocarbon source gases (such as CH_4, C_2H_2, etc), are deposited on the surface of catalyst particles. Then a physical absorption of carbon atoms occurred. After carbon absorption, saturated carbon film will be formed from the continuous decomposition of source gas. The catalyst and substrate surfaces were saturated with carbon layers [2.40].

(3) Thirdly, catalyst was pushed upward due to the diffusion and weak interaction between metal and substrate. Core is formed below catalyst particle because the C atom is not fast enough to diffuse. After the wall of carbon nanotube was formed and rolled up in spherical and cylindrical shapes, hollow carbon nanotubes grown.

(4) Finally, random CNTs and other defective carbon materials are anisotropically

17

etched by plasma. In the meantime, vertically aligned CNTs due to the crowing effect, which suffering less etching, were lengthening by continuous carbon species supplied and diffused into the growing carbon nanotubes.

2.3.1.2. Base-growth model and Tip-growth model

According to the different interaction force between catalyst and substrate, there would be two growth models:

(1) Without buffer layer: because the formation of the silicide on the Si substrate ,the adhesion force between the catalyst and substrate was enhanced . As a result, the growth of CNTs follows the base-growth model.

(2) With buffer layer: the existence of buffer layer reduced the formation of the silicate, it, in turn, reduced the adhesion force between catalyst and substrate, and the mechanism is tip-growth model. Figure 2.6 shows the schematic drawing of the growth mechanism.
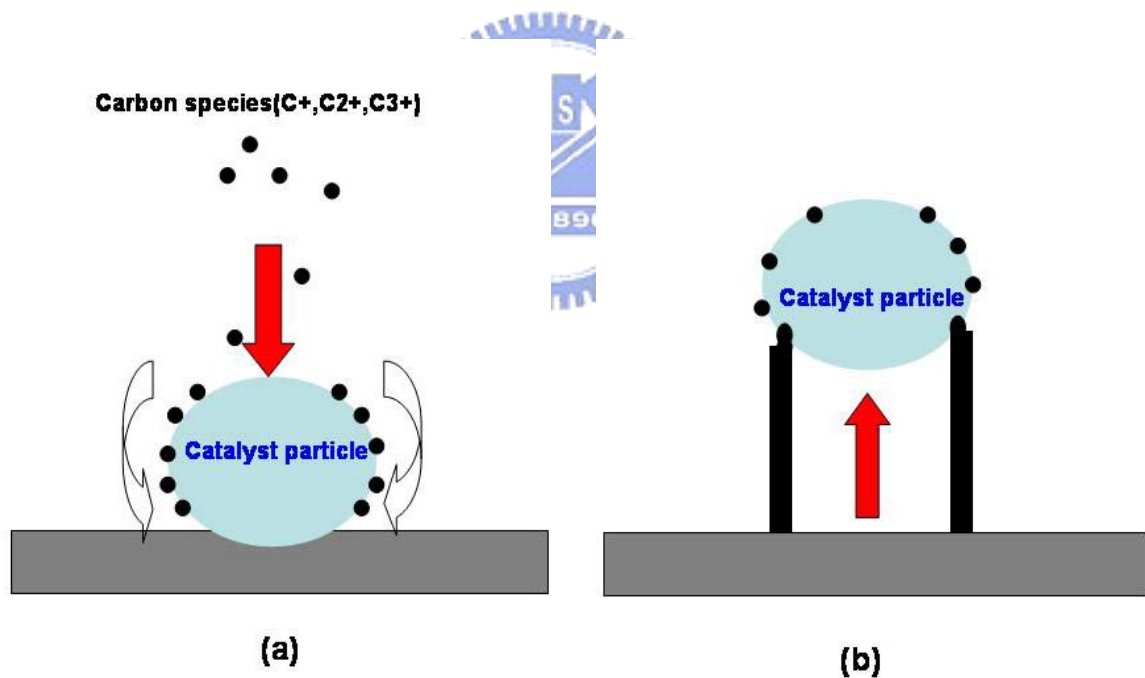
Figure 2.6: Schematic illustration of the growth mechanisms (with catalyst).(a)carbon species diffusion through the catalyst (b) catalyst particle was pushed upward due to the diffusion and weak interaction between metal and substrate ,ex, tube lengthening.

2.3.2. Open-end and close end growth model

Open end growth model was first introduced by Iijima in 1991. He believes that the initial structure of carbon nanotube were clusters with one end opened .Because of the

C2 dimer and C3 trimmer added to the edge of the cluster, the wall of CNTs could be longer and longer. Similarly, the close end growth model demonstrates that the growth of CNTs were due to the direct addition of C2 dimer to the fullerene structure.

2.4. Field emission

2.4.1. Field emission theory

Electron field emission is defined as quantum mechanical tunneling phenomenon. In that electrons extracted from the conductive solid surface, such as a metal or a semiconductor, when the surface electric field is high enough. If a sufficient electric field is applied on the emitter surface, electrons will be emitting through the surface potential barrier into vacuum, even at a very low temperatures. In contrast, thermionic emission is the hot electron emission at high temperature and relatively low electric field. Fig. 2.7(a) demonstrates the band diagram of a metal-vacuum system. Here W0 is the energy difference between an electron at rest outside the metal and an electron at rest inside the metal, whereas Wf is the energy difference between the Fermi level and the bottom of the conduction band. The work function φ is defined as φ = W0 - Wf. If an external bias is applied, vacuum energy level is reduced and the potential barrier at the surface becomes thinner as shown in Fig 2.7(b) [2.41]. Then, an electron having energy "W" has a finite probability of tunneling through the surface barrier. Fowler and Nordheim derive the famous F-N equation (1.1) as follow:

$$J = \frac{aE^2}{\phi t^2(y)} \exp(-b\phi^{\frac{3}{2}} \upsilon(y)/E) \tag{1.1}$$

where J is the current density (A/cm^2).

E is the applied electric field (V/cm),

φ is the work function (in eV),

a = 1.56×10^{-6},

b = -6.831×10^{-7},

y = 3.79x10^{-4}×10^{-4} E$^{1/2}$/φ, t^2 (y)~1.1

These numbers, including a,b, and y, are universal.

Substituting relationships of J = I/α and E = βV into Eq.(1-1), with α being the effective emitting area and β being the local field enhancement factor of the emitting surface, the following equation can be obtained

$$I = \frac{A\alpha\beta^2 V^2}{\phi t^2(y)} \exp\left[-bd\upsilon(y \frac{\phi^{\frac{3}{2}}}{\beta V})\right] \tag{1.2}$$

Taking logarithm on both sides with v(y) ~ 1

$$\log\left(\frac{I}{V^2}\right) = \log\left[A\frac{\alpha\beta^2}{\phi t^2(y)}\right] - 2.97 \times 10^7 \left(\frac{bd\phi^{\frac{3}{2}}\upsilon(y)}{\beta V}\right) \qquad (1.3)$$

the slope of a Fowler-Nordheim (F-N) plot is given by

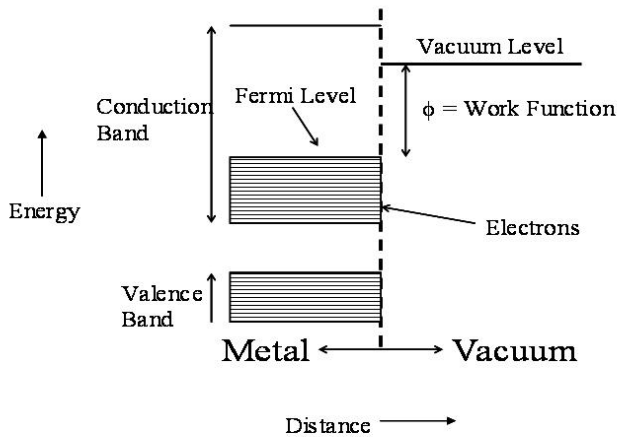$$S = slope(F-N) = bd\left(\frac{\phi^{\frac{3}{2}}}{\beta}\right)$$

Figure 2.7(a) : Schematic representation of the band diagram of a metal/vacuum system. Dashed line: the interface between metal and vacuuystem and Φ is equal to (E vacuum-E Fermi-level) [48].
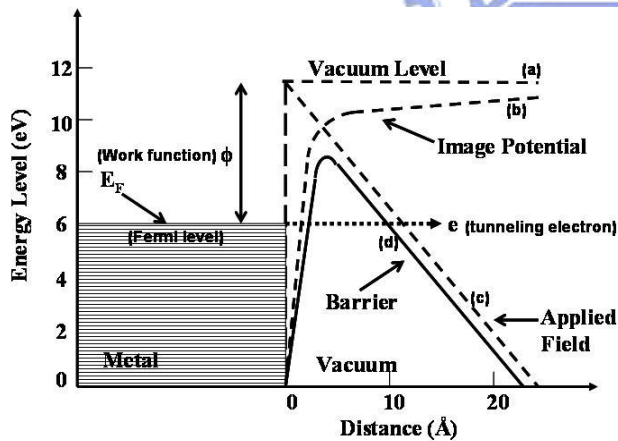
Figure 2.7(b):Sketch of the band diagram of a metal vacuum system under applied field. Dashed line (a): initial energy level of vacuum without applied field. Dashed line (b): potential energy due to micro mirror image force. Dashed line (c): band winding due to external field. Dashed line (d): final band of the vacuum level under applied field. Because of the winding of the band diagram, electrons got more possibility to tunnel through the barrie

2.4.2. Parameter that effect the emission property of CNTs

Carbon nanotubes possess the fowlling properties favorable for emitters (1) high aspect ratio, (2) small radius of curvature at their tips, (3) high chemical stability, (4) high mechanical strength. Due to these extreme properties, nanotubes are under inverstigation toward several application, including electron fielder emitters, probes of scanning type microscopes, gas/hydrogen storage materials, electrode materials of

secondary batteries, and capacitors, and so forth. It has been proved that films of both SWNT and MWNT are excellent field emitters [2.17-2.20]. Nanotubes can be grown in situ with emitting surface. Both nanotubes grown with catalyst and without catalyst shows the same excellent emission property. Field emission parameter for nanotubes varies. The fower-Nordheim equation states that field emission current from a metal tip applied a local field at the tip. Nanotubes field-emission tend to follow the equation [2.17-2.18].

It is still unclear whether the sharpness of nanotubes is their only advantage over other emitters, or if intrinics properties also influence the emission performance. Some reports believe that the large amplification factor, arising from radous of curvature of the nanotubes tips, is partly responsible for the good emsssion characteristics. Detail parameters that would influence the field emission characteristics of nanotubes are summarized in table 2.5.

Table 2.5: *Parameter that effect the dield emission property of carbon nanotube*

Parameter	
Fabrication method	Arc Discharge/Laser Ablation/Thermal CVD, Plasma CVD
Geometrical features	SWNT or MWNT Diameter distribution Length distribution Density distribution Chirality
Orientation / Microstructure	Aligned or non-aligned Straight or curved Cleanliness or Defect Closed-ended or Open-ended With or without catalyst on tips
Density	Low(107cm-2)/Midium(108~109cm2)/High($\geqq$ 109cm-2)
Atmosphere	吸附氣體、 chamber temperature and pressure
Post-treatment	Plasma, laser irradiation, ion bombardment, anneal,…..)

2.5. Field emission enhancement of carbon nanotube

Field emission current of cnt films depends strongly on the work function and geometry of the surface of the films. To enhance the field emission properties of CNTs, some effective methods are used to treat the surface of CNTs. Table 2.6 showes recent developments in treatment for CNTs film. Many factors would reduce the field emission performce of nanotubes, including metalparticle on the tip [2.19-2.21], amorphous carbon(a-C) cover over the nanotubes [2.22], adhersion between nanotubes and substrate under applied extremely high field [2.23-2.25]. Depending on the methods to purify the nanotubes, post-treatments are classified into several categories:

(1) plasma etching: including Ar, He (non –reactive physical plasma), NH3(reactive chemical plasma) [2.27-2.34]

(2) thermal treatment :including annealing, oxidation [2.35]

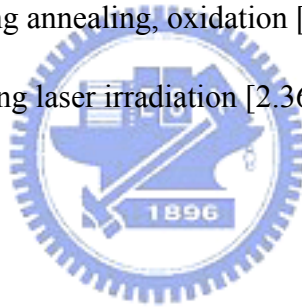(3) physical treatment: including laser irradiation [2.36].

Table 2.6: *Field enhancement of carbon nanotube*

Year	Process	Substrate	Source gas	Catalyst	Temperature ℃	Bias	Growth Time (min)	Result	Density (/cm2)	I_D/I_G	Enhancement factor(β)	Turn-on voltage (V/μm)	Journal	Author
2004	CVD	Quartz glass	Ferroence-xylene-argen hydregn	Fe	700		30	VA-MWCNT	$6(+-3)*10^6$				Science	Beuce J.Hinds
2004	Rf-PECVD	Soda-line Glass	C_2H_2/NH_3	Ni100nm/Cr30nm	<500	Dc	5~15	VA-CNT		3.4-4.0	6700~9800		MCP	Y.Shiratori
2004	Dc-PECVD	Si	C_2H_2/NH_3	Ni3nm/SiO$_2$50nm	550-700		15	VA-CNT film					JAP	C.Ducati
2004	Dc-PECVD	Si	C_2H_2/NH_3	Ni/Cr				VA-MWCNT	$1*10^6$~$6*10^6$				APL	S.Hjo and Y.Tu
2004	RF-PECVD	Metallic	C_2H_2/NH_3	Ni(sol-gel)	700~800		5	Individual-VACNT					APL	M.Mauger
2004	Dc-sputtering	Si		Ni10nm	700	Dc	3	VA-CNT	$1*10^9$~$.2*10^9$			4.63	DRM	K.Y Lee
2003	PECVD	Si	C -powder	Fe(NO$_3$)$_3$/SiO$_2$	900+-10		15	VA-CNT boundles					CPL	S.Orlanduci
2003	PECVD	Si	Ch$_4$	Ni20nm	600	Dc		VA-CNT					DRM	Q.Yang
2003	MW-PECVD	Si	CH$_4$	Ni	550								DRM	S.G Wang
2003	PECVD	Si		Ni3.5nm-7nm				VACNT					JMPS	H.J Qi
2003	Pyrolyz	Si	FeC$_{32}$N$_8$H$_{16}$	FePc/Copc/NiPc	700-1000		20	VACNT	$>10^{10}$	0.66~0.87			JPCB	Nam Seo Kim
2003	Dc-bias ering	Si		Ni100A	700	Dc		VACNT	$1*10^9$				ASS	Nobyuki Hayashi
2003	Injection CVD	Quartz	Ferrocence-toluene	Fe	550-940		60	VA-MWCNT	$1*10^9$	0.4(800C)			Carbon	Charanjeet

2003	Dc grow discharge CVD	Plastic(Kapton polyamide foil polymides)	C_2H_2/NH_3	Ni6nm/70nmCr	200	Dc		VACNF			850	3.2-4.2		
2002	PECVD	Si	C_2H_2/NH_3	Ni10nm/Ti10nm	700		10	VACNF					APL	Vladimir L.M
2002	PECVD	Ti	C_2H_2/NH_3	Fe/Ni/Co			10	VACNT					APA	Z.P.Huang
2002	PECVD	Si											APA	Z.P.Huang
2001	CVD	Si	Ch_4	Co5nm	800	Dc	15	VA-CNT					APL	Y.Avigal
2001	CVD	Si	Ch_4	Fe	300	Dc	30	VA-CNT					APA	M.sveningsson
2001	Pyrolysis	Glass		FePc	950		2~60	VA-MWT					CPL	X.ianbao
2001	Dc-PECVD	Si	$C2H_2/NH_3$	Ni/SiO$_2$/Si	1000		10	VACNT					JAP	M.Chhowalla
2001	PECVD	Si	C_2H_2/NH_3	Fe/Co/Ni				VACNT					APL	Y.H.Wang
2000	MW-PECVD	Si	C_2H_2/NH_3	Co2nm	825	Dc	10	VA-MWNT	$4.4*10^9$				APL	Chris Bower
2000	PECVD	Si	C_2H_2/NH_3	Ni(0.5nm~20nm)/SiO$_2$50nm	750	Dc	15	VACNT					APL	C.Bower.W.Zhu. S.Jin
2000	PECVD	Glass	C_2H_2/NH_3	Ni	<600	Dc	14	VA-MWCNT				1.5	APL	Jae-hee Han
1999	CVD	Si		Fe				VACNT				4.8~6.1	Science	S.Fan.H.Dai
1999	MW-PECVD	Si	Ch_4	Co	700	Dc	2-11	VACNT					APL	S.H Tasi
1999	CVD	Si		Fe	700	Dc		VACNT					Science	Shoushan
1998	CVD	Galss		Ni	700		5-25	VACNT					Science	Z.F.Ren
1996	CVD	Si		Fe	700			VACNT					Science	W. Z. Li, S. S. Xie,

Table 2.7: *Field enhancement of carbon nanotube*

Process	Journal	Effect
Adsorbates	Applied surface science 233(2004)20-23	Increase fe current "2"order of magaitude(mwnt
	Diamond and related materials13 (2004)1306-1313	Gas molecule acts as tunneling states for electrons emittings from the nanotube tip into to the vacuum
Plasma etching	Applied surface science225(2004)380-388	1.Turn-on field(0.1 μA/cm2) decrease from 3.9 to 1.5V/μm after HP(hydrogen plasma) treatment(mwnt) 2.Spot density is 1.5x104cm-2 at field 5.2V/μm
	Diamond and related materoals13(2004)54-59	1.Field electron emission density increase from 103 to 106cm-2 CNT become nodular after HPP(hydrogen plasma process) 2.lighting spot become uniform and smaller after HPP
	Diamond and related materials	1.Needle –shaped boundles on the surface of CNTs is found 2.FE property is enhanced after Ar and O2 plasma treatment
	Surface coating and Teacnology179(2004)63-69	1.CNTs with HP treatment are covered carbon nano particles and have low turn-on voltage0.5V/μm(at 0.1 μ/cm2),high emission site spot density(ESD)104cm-2 ,high emission density 10mA/cm2 (at 7.5V/μm)
	Chemical physics letters373(2003)109-104	1.CNTS coverd carbon nanoparticles after HP 2.Low turn-on voltage 0.5V/ μm (at 0.1 μA/ cm2) 3.High emission sopt density(ESD)104/ cm2
	Thin solid films444(2003)64-69	1.0.305mA(at 2V/ μm) 2.Turn-on field 1.7 V/ μm
Laser irradiation	Diamond and related materials13(2004)1004-1007	1.FE current density at 2V/μm is enhanced from 0.75 to 14.0mA/cm2 (MWNT) 2.CW laser(633nm,5mm spot size)incident onto CNTS "during" measuring FE current
Heavy ion radiation	Diamond and related materials13(2004)221-225	1.FE current improved due to the formation of conductive trigonal carbon nano-channels within the tetragonally-boned carbon matrix
	Chemical physics letters378(2003)232-237	1.Increase defectsand and decrease turn-on field after Ar ion irradiation

Table2.8: *Vertical-aligen carbon nanotube*

Process	Journal
Embedding catalyst nano-paraticles	• Science.vol 303.62 (2003) • Science.vol 283.512(1999) • Science Vol274.1701(1996)
Utilizing very dense tube growth which forces the tubes to align parallel to each other	• J.Appl.Phys.91-3847(2002) • Chem.Phys.Lett.303-467(1999) • Chem.Phys.Lett340-419(2001)
Growth under plasma conditions and/or by application of a bias voltage to the substrate	• Diamond.Rel.Materrials.13.1228-1231(2004) • Material.Ahem.Phys.87.31-38(2004) • Applied Surface science.212.393-396(2003) • Diamond.Rel.Materrials.12.2175-2177(2003) • Diamond.Rel.Materrials.12.1482-1487(2003) • Chem.Phys.Lett.367-109(2003) • Appl.Phys.Lett.80.4816-4818(2002) • Appl.Phys.Lett.80-4816(2002) • Nanotechnology.13-62(2002) • Vac.Sci.Technol.A.19-1796(2001) • Appl.Phys.Lett.78-2291(2001) • Appl.Phys.Lett.78.2291-2293.(2001) • J. Appl.Phys.90.5308(2001) • Appl.Phys.Lett76-2469(2000) • J. Appl.Phys.88-7363(2000) • Appl.Phys.Lett.77-830(2000) • Science.283.512(1999) • Science.282.1105(1998) • Appl.Phys.Lett.74-3462(1999)
Diract incoming of the flux of carbon source	• Chem.Phys.Lett.367-109(2003)
Effect of the kind of catalyst which contribuate to VA-CNT growth	• Appl.Phys.A.74.387~391(2002) • J.Chem.Phys.B.107.9249-9255(2003)

Reference

[2.1] J.W. Mintmire , and C.T White, Carbon 33, 893 (1995) .

[2.2] M.F. Yu, O. Lourie, M.J. Dyer, K. Moloni, T.F.Kelly, and R.S.Ruoff, Ssience 287, 637 (2000).

[2.3] P.Poncharal, Z.L.Wang, D. Ugrate, and W.A. DeHeer, Science 338,678 (1996).

[2.4] M.M. Treacy, T.W. Ebbesen, and J.M. Gibson, Nature 38, 678 (1996).

[2.5] D.S. Bethune, C.H.Kiang, M,S. Devries, G. Gorman, R. Savoy ,and R. Beyers, Nature 63, 576 (1993).

[2.6] C. Journet, E.K. Maser, P. Bernier, A. Loiseau, M. Lamy de la Chapelle, S.Lefrant, P. Deniard, R. Lee, and J.E. Fischer, Nature 388,756 (1997).

[2.7] A.Thess,R.Lee,P.Nikolave,H.Dai,P.Petit,J.Robert,C,Xu,Y.H.Lee,Kim,A. G.Rinzler,D,T.Colbert,G.E.Seuseria,D.Tomanek,J.E.Ficher,   and   R.E.Smalley. Science 273,483 (1996).

[2.8] H.O. Pierson, "Handbook of Chemical Vapor Depostion"(Noyes Publication, Park Ridge,Nj,1992).

[2.9] M.J. Hampden-Smith and T.T. Kodas, Chem.Vapor.Depostion 1, 8 (1995).

[2.10] J.H. Hafner, M.J. broniKowski, B.R. Azamian, P. Nikolave, A.G. Rinxler, D.T. Colbert, K.A. smith, and R.E.Smalley, Chem.Phys.Lett.296, 195 (1998).

[2.11] A.M. Casell, J.A. Raymakers, J. Kong, and H.J. dai,I. Phys.Chem.B 103, 6484 (1999).

[2.12] J.F. Colomer, C. Stephan, S. Lefrant, G. V.Tendeloo, I.Willems, Z.Konya,A. Fonseca, C. Laurent, and J.N. Nagy, Chem.Phys.Lett 2, 525 (2002).

[2.13] Q.W. Li, H. Yan,Y. Chang Zang, and Z.F. Liu, J.Mater.Chem.12,91 (2003).

[2.14] P. Nikolaev, M.J. Bronikowski, R.K. Bradley, F. Rohmund, D.T. Colbert, K.A. Smith and R.E. Smalley, Chem.Phys.Lett 313,91 (2002).

[2.15] M.J. BroniKowski, P.A. Willins, D. Tcolbert, K,A. Smith, and R.E. Smalley,

J.Vac.Sci.Teacnol A19,1800 (2002).

[2.16] S.Maruyama,R.Kojima,Y.Miyauchia,S.Chiashia, and
M.Kohno,Chem.Phys.Lett.360

[2.17] W.A. De Heer, A. Chatelain, and D. Ugrate, Science 270,1179 (1995).

[2.18] J. Bonard, J. Salvant,T, Stockli,W. de Heer, L. Forro, and A. Chatelain,
Appl.Phys.Lett.   73, 918 (1998).

[2.19] J.M. Bonard , J.P. Salvetat, and T. Stockli, Applied Physics A 69,245 (1999).

[2.20] Yahachi Saito and Sashiro Uemura .Carbon 38 , 169 (2000).

[2.21] Q. H. Wang et al, Appl. Phys. Lett   70, 3308(1997).

[2.22] M. Yumura et al, Diamond Relat. Mater. 8, 785 (1999).

[2.23] Y. Saito and S. Uemura, Carbon 38, 169(2000).

[2.24] C. C. Chaung et al, Diamond Relat. Mater. 13, 1012(2004).

[2.25] Y. Zhang et al, Appl. Phys. Lett. 79, 3155 (2001).

[2.26] V. I. Merkulov et al, Appl. Phys. Lett. 80, 4816. (2002).

[2.27] M. Meyyappan et al, Plasma Sources Sci. Technol. 12, 205 (2003).

[2.28] S. C. Kung, K. C. Hwang, and I. N. Lin, Appl. Phys. Lett. 80, 4819 (2002).

[2.29] M. Yudasaka et al, Carbon 41, 1273 (2003).

[2.30] Adolfo Gonzalez-Berrious .Diamond and Related Materials 13, 221 (2004).

[2.31] Yuming Liu and Liang Liu. Diamond and Related Materials 13, 1609 (2004).

[2.32] Ke Yu and Ziqang Zhu. Surface and Coatings Technology 179, 63 (2004).

[2.33] Ke Yu, Ziqang Zhu .Applied surface Science 225, 380 (2004).

[2.34] K.S. Yeong, J.T.L. Thong, Applied Surface Science 133, 20 (2004).

[2.35] Do-Hyung Kim, Hoon-Sik Jang, and Chang-Duk Kim, Chemical Physics
Letters 378, 232 (2003).

[2.36] Kyung Soo Ahn, June Sik Kim. Carbon 41, 2481 (2003).

[2.37] Sheng-Chin Kung and Kuo Chu Hwang. Applied Physics Letters 80, 4819 (2002).

[2.38] I-Nan Lin .Diamond and Related Materials 13, 1004 (2004).

[2.39] T.W. Ebbeson, "Carbon Nature Preparation and Properties", CRC Press,1997.

[2.40] R.H. Fowler and L.W. Nordheim, Proc. R. Soc. London A (1928).

[2.41] R.H. Fowler and L.W. Nordheim, Proc. R. Soc. London A (1928).

[2.42] M.S. Dresselhaus, G. Dresselhaus, P.C. Eklund, "Science ofFullerenes and Carbon nanotubes", San Diego:Academic Press,1996.

[2.43] W. Kratschmer, L.D. Lamb, K. Fostiropoulos, and D.R. Huffman, Nature 347, 354(1990).

[2.44] R. Smalley, Science 273, 483(1996).

[2.45] A.M. Cassell, J.A. Raymakers, J. Kong, and H.J. Dai, J. of Phys. Chem. B. 103, 6484(1999).

[2.46] 蕭清松, 黃文亮, 黃廷位, 機械工業雜誌 255,106(2004).

[2.47] Baker and Harris, Chemistry and Physics of Carbon 14, (1978).

[2.48] R. H. Fowler, and L. W. Nordheim, (1928) Proc. R. Soc. London A.